Sensors & Transducers, Vol. 27, Special Issue, May 2014, pp. 127-136

Sensors & Transducers

http://www.sensorsportal.com

Immunosensors Based on Single-Walled Carbon Nanotubes (SWCNT) for the Detection of Deep Venous Thrombosis

[1, 2, 3] Sondes BOURIGUA, [2] Abderrazak MAAREF, [1] Abdelhamid ERRACHID, [1] François BESSUEILLE, [1, *] Nicole JAFFREZIC-RENAULT

[1] University of Lyon, Laboratory of Analytical Sciences, UMR-CNRS 5180, Claude Bernard University, Lyon I, 43 Boulevard du 11 Novembre 1918, 69622 Villeurbanne Cedex, France
[2] University of Monastir, Laboratory of Adanced Materials and Interfaces, Faculty of Sciences of Monastir: Avenue of environnement, 5019 Monastir Tunisie
[3] Laboratoire Méthodes et Techniques d'Analyses-INRAP, 2020-Ariana Tunisie
*Tel.: +33472431182, fax: +33472431206
E-mail: Nicole.jaffrezic@univ-lyon1.fr

Received: 31 December 2012 /Accepted: 10 August 2013 /Published: 26 May 2014

Abstract: Thanks to their properties, Single-Walled carbon nanotubes (SWNT) open a new way to the fabrication of Immunosensors with the particularity to amplify the response signal from antibody–antigen interaction and to improve the Immunosensors characteristics. In this context, two new impedimetric immunosensors were developed by immobilizing antibody on Single-Walled carbon, the later was immobilized following two ways the first consist of immobilizing the carbon nanotubes on a polypyrrole layer by adsorption and the second consist of functionalized gold with amino thiol and then immobilizing the carbon nanotubes with covalent binding. The electrical properties and the morphology of the immunosensors have been characterized respectively by Electrochemical Impedance Spectroscopy, cyclic voltammetry and Atomic Force Spectroscopy. A low detection limit for both immunosensors was determined as 1 pg/ml and linear ranges up to 10 ng/ml with polypyrrole and up to 100 ng/ml with amino thiol were obtained. Moreover, the studied Immunosensors exhibited high sensitivity, stability and reproducibility. *Copyright © 2014 IFSA Publishing, S. L.*

Keywords: D-dimer, Carbon nanotubes, Impedance spectroscopy, Polypyrrole, Amino thiol.

1. Introduction

Deep venous thrombosis (DVT) is clotting of blood in a deep vein of an extremity (usually calf or thigh) or the pelvis. DVT is the primary cause of pulmonary embolism. DVT results from conditions that impair venous return, lead to endothelial injury or dysfunction, or cause hypercoagulability. DVT may be asymptomatic or cause pain and swelling in this extremity. Diagnosis is by history, physical examination, and duplex ultrasonography or other testing as necessary [1].

The D-dimer test has an important role in the diagnostic approach to deep venous thrombosis (DVT). D-dimer fibrin fragments are present in fresh fibrin clot and in fibrin degradation products of cross-linked fibrin. Monoclonal antibodies specific for the D-dimer fragment are used to differentiate fibrin-

specific clot from non–cross-linked fibrin and from fibrinogen. These specific attributes of the D-dimer antibodies account for their high sensitivity for venous thromboembolism. [2] Reference concentrations of plasma D-dimer (usually <0.50 μg/mL) are a useful negative predictor to rule out venous thromboembolism in patients [3].

In this study, we propose a new biosensor for D-Dimer detection, based on carbon nanotubes. Since the discovery of carbon nanotubes in 1991 by Iijima [4], carbon nanotubes have received much attention for their many potential applications such as ultra-strong wires, nanoelectronic devices, field electron emitters, nanocomposite materials, and more [4, 6]. Carbon nanotubes exhibit excellent mechanical, electrical, thermal and magnetic properties [6]. The exact magnitude of these properties depends on the diameter and chirality of the nanotubes and whether they are single-walled or multi-walled form. Advances in the synthesis of multi-walled (MWNTs) and single-walled carbon nanotubes (SWNTs) continue to rapidly improve both their quality and quantity, and reduce cost due to their high accessible surface area, chemical stability, high conductivity and low mass density. They enable new applications of materials containing carbon nanotubes.

Single-walled carbon nanotubes are cylindrical graphene sheets with diameters of about 0.7–2 nm and lengths of up to several microns. Due to the geometry of these carbon nanotubes, this material has an impressive high specific surface of more than 1000 square meters per gram [7] by considering the formation of small bundles. The specific surface makes this material a promising candidate for the construction of highly porous three dimensional nanostructured frameworks. Also combination of carbon nanotubes and polymers has attracted considerable attention in biosensor field. Experimentally introducing CNTs into a polymer matrix could significantly improve the mechanical and electrical properties of the neat polymer matrix [8, 9]. Many reports have also shown that the formation of polymer/CNT composites can be considered as a useful approach for the fabrication of polymer-based devices. [10, 11]

Among conducting polymer, polypyrrole (PPy) was used in synthesizing polymer/CNT composites due to its environmental stability and excellent electrical conductivity [12, 13]. PPy can be prepared by chemical or electrochemical oxidation of pyrrole in various organic solvent and in aqueous media [14–15]. Electrochemical polymerization leads to formation of a conductive PPy thin film on the working electrode. For instance, Single-walled carbon nanotubes (SWCNTs) have been incorporated in polypyrrole matrices via functionalization like oxidation of the nanotubes sidewalls for introducing carboxylic acid groups.

In this context, we report two systems of impedimetric immunosensors based on Single-Walled Nanotubes (SWCNT-COOH) for the detection of Deep Venous Thrombosis: the first one consists of immobilizing the carbon nanotubes by adsorption on a polypyrrole layer synthesized by chronoamperometry on gold and the second consist of functionalized gold with amino thiol for immobilizing the carbon nanotubes by covalent attachment between the functionalities NH_2 of amino thiol and the functionalities COOH of carbon nanotubes.

The anti-D-dimer reduced antibody was immobilized on the surface of the carbon nanotubes functionalized with COOH which is previously linked to polypyrrole film or amino thiol. EIS technique was firstly used, to study the electrical properties of the biolayer and then, to monitor the formation of the Immunosensors membrane and the recognition of specific antigen by the antibody bonded to carbon nanotubes.

2. Experimental

2.1. Reagents

The gold electrodes were fabricated by evaporation of gold layer of 300 nm thickness on silicon substrate using a titanium layer as adhesion layer of 30 nm thicknesses. These gold electrodes were provided by the LAAS, CNRS Toulouse, France.

Pyrrole monomer (Sigma) was previously distilled prior to use, Lithium Perchlorate ($LiClO_4$), Acetonitrile were obtained from Fluka.

The anti-D-dimer reduced antibody (Fab fragment hyst-ScAc) and the D-dimer antigen were obtained from Wyeth Company. Single-Walled Carbon Nanotubes (SWCNT-COOH) (ref DRP-CNT sol), were provided by DROPSENS, Spain. 11-amino-1-undecanthiol was obtained from Sigma Aldrich. N-(3-dimethylaminopropyl)-N'-ethyl-carbodiimide hydrochloride (EDC), N-hydroxysuccinidmide (NHS) and sodium dodecyl sulfate salt (SDS), used as surfactant was provided by Sigma–Aldrich.

The buffer solution used for all experiments was Phosphate Buffer Saline (PBS) pH7.0. All solutions were made up in ultrapure water (resistance 18.2 MΩcm−1) produced by a Millipore Milli-Q system.

2.2. Instrumentation

2.2.1. Cyclic Voltammetry (CV)

Cyclic voltammetry and amperometric measurements were performed in a conventional three electrode cell configuration consisting of a working gold electrode (0.11 cm^2), a saturated calomel reference electrode (SCE) and a platinum plate (0.5 cm^2) as a counter electrode. All cyclic voltammetry experiments were performed using a

Voltalab 80, model PGZ 402, controlled by a software (Voltamaster 4) from Hach Lange France SAS, Marne-la Vallee. The electrochemical measurements were performed in an 8 mM PBS buffer at pH 7.0 with 1mM $Fe(CN)_6^{3/4-}$ at room temperature (21 ± 3°C). A potential range of -0.5 to 0.7 V was applied with a scan rate of 100 mV/s.

2.2.1. Electrochemical Impedance Spectroscopy (EIS)

The electrochemical impedance measurements were performed using Voltalab 80, Model PGZ 402. The instrument was used in a three-electrode cell configuration as described before. The impedance spectroscopy measurements were carried out in the frequency range from 0.05 Hz to 100 kHz using a modulation voltage of 10 mV. Measurements were performed in a PBS buffer solution at pH 7.0. The measured impedance spectra were analyzed in terms of electrical equivalent circuits using the analysis program Zview (Scribner Associate Inc, Southern Pines, NC, USA).

2.2.2. Atomic Force Microscopy (AFM)

Atomic force microscopy (AFM) experiments were performed in air, using a Pico Plus Agilent/Scientec microscope with a 10 μm scanning head. The images were registered in "tapping" mode using silicon tips. The average resonance frequency of the tips was 300 kHz. The images presented in this paper were acquired with a resolution of 512×512 pixels and were processed by means of a plane fit. The scanned area size was 1 μm×1 μm.

2.3. Preparation of the Immunosensor Based on SWNCT-COOH/ Polypyrrole (system 1)

2.3.1. Electropolymerization of the PPy Film on Gold Electrodes

In order to control the thickness of the copolymer film, chronoamperometry technique was chosen for the film electrodeposition on the gold electrode. Before electropolymerization, the gold surface was cleaned in an ultrasonic bath for 10 minutes in acetone, dried under a dry N_2 flow and then dipped for 1 minute into "piranha solution" composed of 9:3 (v/v) 98 % H_2SO_4/30 % H_2O_2.

The gold substrate was then 2 to 3 times rinsed with ultrapure water and dried under nitrogen flow. After cleaning, the gold electrodes were immediately placed as working electrode in a three-electrode electrochemical cell. Electropolymerization was performed at 0.9 V/SCE for 2 s in an acetonitrile solution containing 0.1 M pyrrole and 0.5 M $LiClO_4$. The solution was deaerated through nitrogen bubbling for 20 min before use.

The measured charge consumed during the electropolymerization process reached 2.54 10^{-3} C corresponding to a charge density of 13.3 mC cm^{-2}. The polypyrrole film thus obtained is in its electrically p-type conducting state, i. e partially oxidized by the ClO_4^- anion.

2.3.2. Carbon Nanotubes Immobilization

The carbon nanotubes were dispersed in aqueous solution of 0.1 mol/L SDS (sodium dodecyl sulfate). Then SWCNT-COOH (0.17 g/L) was added on polypyrrole film and incubated for 2h at room temperature. Immobilization of carbon nanotubes on polypyrrole was via adsorption by hydrogen linking. These immobilized carbon nanotubes were activated with EDC (0.4 M) /NHS (0.1 M) for 45 min before addition of antibody, to convert the terminal carboxylic groups to an active NHS ester.

2.3.3. Antibody Immobilization

Antibody scAb fragment (0.4 mg/mL) was immobilized on activated carbon nanotubes for 1 h at room temperature by covalent attachment between his terminal amino group NH_2 and activated COOH functionalities of carbon nanotubes: the substrate was then rinsed with PBS.

After antibody immobilization, 20 μL of a casein solution was added to the electrode surface and incubated for 30 minutes at room temperature to block the unreacted and the non-specific sites, and then the substrate was rinsed with PBS.

Then antigen solution with different concentrations was incubated on immobilized antibody for 30 min at room temperature.

2.4. Preparation of the Immunosensor Sed on SWNCT-COOH / 11-Amino-1-Undecanethiol (Amino Thiol) (System 2)

2.4.1. Functionalization of the Gold Electrode with Amino Thiol

The amino thiol monolayer was prepared by soaking a clean gold electrode (Au) in 1 mM 11-amino-1-undecanethiol (AUT) in ethanol solution for 12 hours at room temperature in darkness, washing the electrode thoroughly with ethanol to remove physically adsorbed 11-amino-1-undecanethiol by immersing the electrode in PBS (pH 7).

Then, the 11-amino-1-undecanethiol monolayer was chemisorbed on the gold electrode surface and then functionalized with an array of amino groups towards the solution.

2.4.2. Immobilization of Carbon Nanotubes

Before immobilization of carbon nanotubes on the electrode, 0.17 g/L of the SWCNT-COOH material was dispersed in an aqueous solution of 0.1 mol/L SDS. Then Single Walled Carbon nanotubes (SWCNT-COOH) were activated with a solution containing 0.1 M NHS and 0.4 M EDC for 45 minutes, to convert the terminal carboxylic groups to an active NHS ester.

After activation, carbon nanotubes were immobilized on gold functionalized with amino thiol for 2 hours at room temperature. The substrate was then rinsed with ultrapure water. The carbon nanotubes SWNCT-COOH were attached by covalent binding to the NH_2 functionalities of the amino thiol.

2.4.3. Antibody Immobilization

The anti-D-dimer reduced antibody (Fab fragment hyst-ScAc) (0.4 mg/mL) was incubated on carbon nanotubes for 1 h at room temperature and then a covalent attachment between its terminal group NH_2 and the activated COOH functionalities of carbon nanotubes. The excess of antibodies was removed by rinsing with PBS.

After antibody immobilization, 20 µl of a casein solution was added to the electrode surface and incubated for 30 minutes at room temperature to block unoccupied sites at the surface of the immunosensor.

Then antigen solution with different concentrations was incubated on immobilized antibody for 30 min at room temperature.

3. Results and Discussion

3.1. Recognition and Binding Processes between the Different Layers of the Immunosensor Structure

Scheme 1(a) and Scheme 1(b) show the schematic steps for the formation of the biolayer and the antigen-antibody recognition with the first system and the second system respectively. In the first system, after the electrodeposition of the polymer film carbon nanotubes were adsorbed by hydrogen bonding and the antibody was attached on carbon nanotubes by covalent binding with activated COOH functionalities of carbon nanotubes. In the second system, with amino thiol carbon nanotubes were linked by covalent attachment on amino thiol and the antibody also was linked by covalent attachment on carbon nanotubes.

3.2. AFM Characterization

Fig. 1a and Fig. 1b show the morphology of the polymer film deposited on the gold electrode before and after carbon nanotube immobilization respectively. The high magnification of AFM images revealed a rather rough surface composed of round globular particles with an average diameter of 20-30 nm for the Fig. 1a and 15-20 nm for the Fig. 1b which prove carbon nanotubes immobilization on polypyrrole film, as SWCNT bundles.

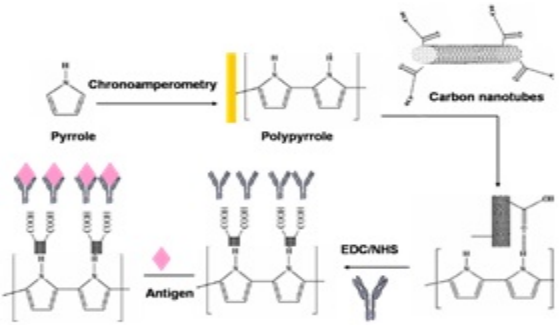

Scheme 1 (a). Schematic representation of the fabrication process of the multilayer system of the Immunosensors on the gold electrode for the first system based on pyrrole.

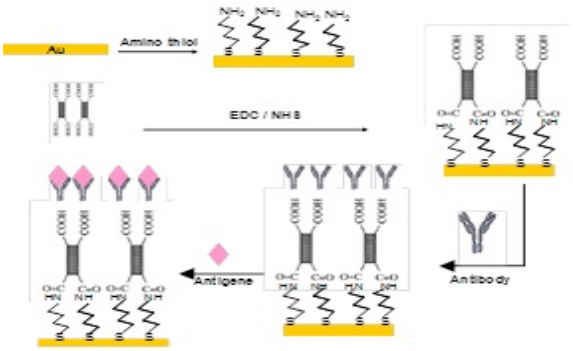

Scheme 1 (b). Schematic representation of the fabrication process of the multilayer system of the Immunosensors on the gold electrode for the second system based on amino thiol.

Fig. 2a and Fig. 2b show the morphology of gold functionalized with 11-Amino-1-undecane thiol before and after carbon nanotubes immobilization respectively. Fig. 2a shows round globular particles with an average diameter of 75 nm, corresponding to gold surface, and Fig. 2b shows smaller round globular particles with an average diameter of 15-20 nm which prove carbon nanotubes immobilization as SWCNT bundles. The length of SWCNT bundles is not observable due to the interaction of the tip with surface and to the initial roughness of gold electrode surface.

3.3. Electrical Characterization of the Biofilm by Cyclic Voltammetry

Modified electrode was electrochemically characterized in 8 mM phosphate buffer solution at

pH 7.0 by cyclic voltammetry with 1 mM Fe $(CN)^{63/4-}$. Fig. 3a and Fig. 3b show the cyclic voltammograms of the gold surface modified by the carbon nanotubes for both systems, with polypyrrole and amino thiol respectively. For both systems voltammograms show an increase in current of oxidation-reduction peaks after SWCNT-COOH immobilization which confirms the attachment of carbon nanotubes on polypyrrole film and on amino thiol and brings out the conducting properties of carbon nanotubes. The SWCNT layer promotes electron transfer through the layer of thiol and polypyrrole and increases the conductivity of the system, and therefore the charge transfer rate.

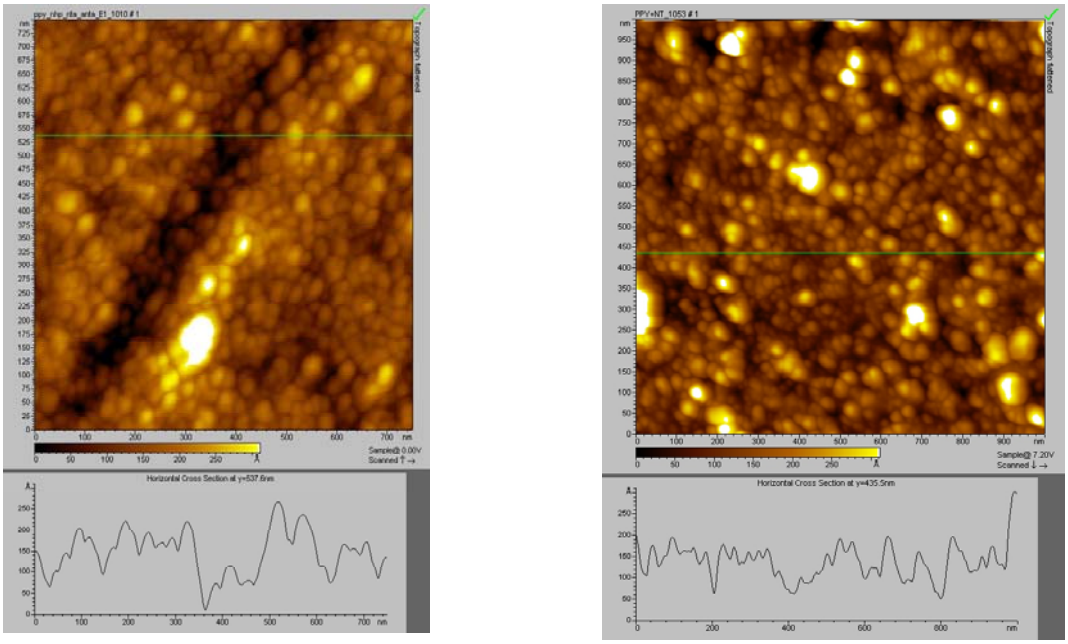

(a) (b)

Fig. 1. (a) AFM image of gold electrode functionalized with the polypyrrole film. (b): AFM image of gold electrode functionalized with the polypyrrole film after SWCNT-COOH immobilization.

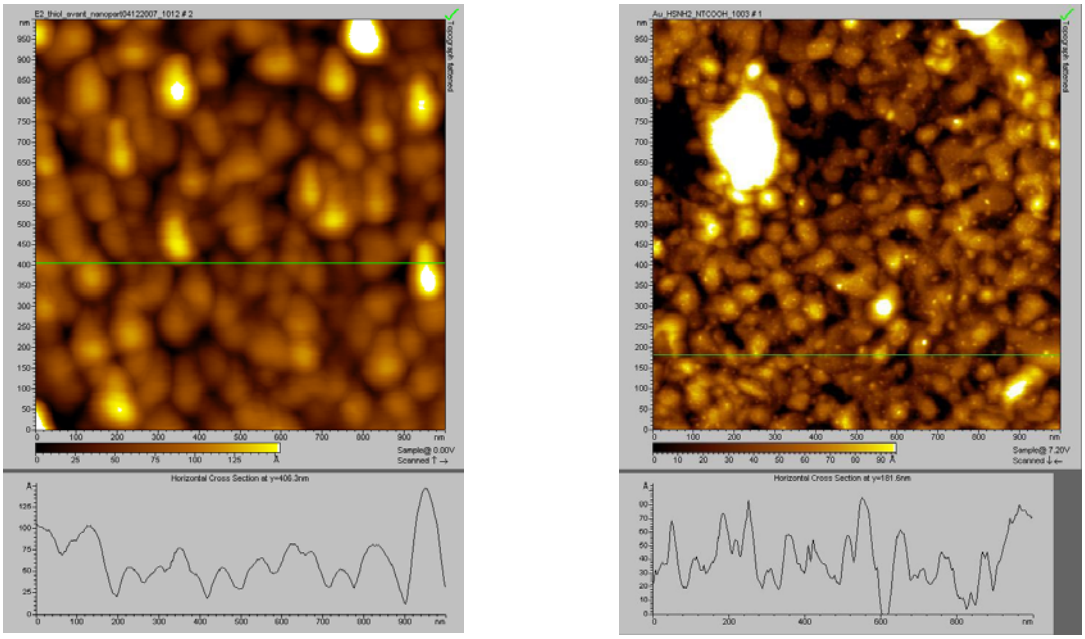

(a) (b)

Fig. 2. (a) AFM image of gold electrode functionalized with amino-thiol. (b) AFM image of gold electrode functionalized with amino-thiol after SWCNT-COOH immobilization.

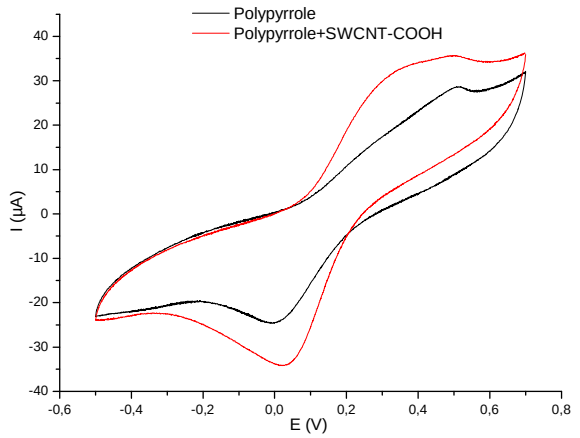

(a)

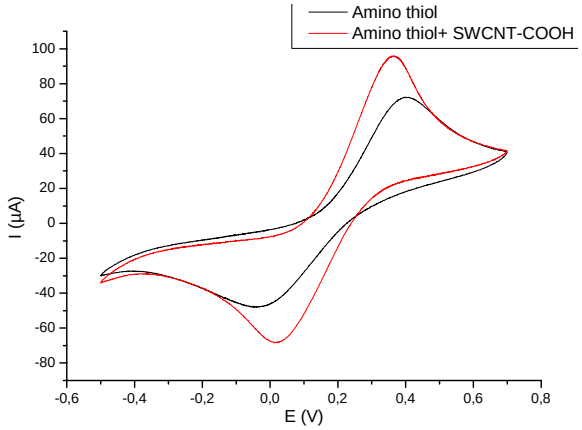

(b)

Fig. 3. (a) Cyclic voltammograms corresponding to (a) polypyrrole film and (b) polypyrrole + carbon nanotubes in PBS pH 7.0 with the redox couple. Scan rate 100 mV/s, (b) Cyclic voltammograms corresponding to (a) Amino thiol (b) Amino thiol + carbon nanotubes in PBS pH 7.0 with the redox couple. Scan rate 100 mV/s.

3.4. Electrical Characterization of the Biofilm by Impedance Spectroscopy

EIS was used to control the building-up of the biofilm in the PBS (pH 7.0) at -1.2 V potential for the first system with polypyrrole. Fig. 4a shows the results of impedance spectroscopy measurements as Nyquist plots, for the assembly of the biofilm on gold electrode.

The Nyquist plot shows that the interfacial impedance decreases after carbon nanotubes immobilization on polypyrrole layer, which proves that carbon nanotubes increase the conductivity of the electrode/electrolyte interface. Then the attachment of the antibody leads to a decrease of interfacial impedance. The increase of CNT conductance was already observed after adsorption of negatively charged protein, this protein being placed inside the Debye length. A little increase of the interfacial impedance is observed after casein addition, due to the big size of casein.

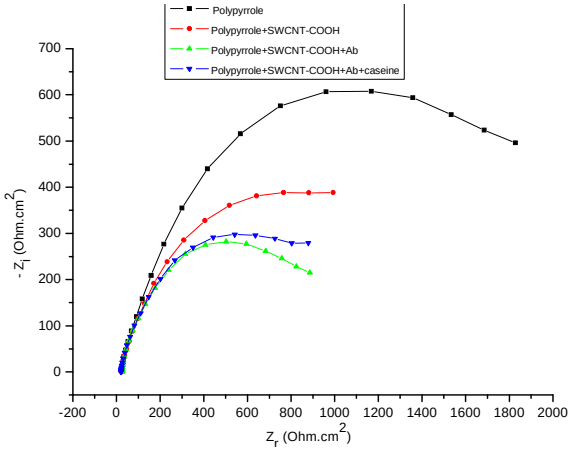

Fig. 4 (a). Nyquist diagram (-Im (z) vs. Re (z)) for the impedance measurements (at -1.2 V) vs. SCE in PBS solution (pH 7.0) corresponding to the various layers grafted onto the gold electrode: (a) polypyrrole film; (b) polypyrrole+ carbon nanotubes; (c) polypyrrole + carbon nanotubes +Antibody; (d) polypyrrole +carbon nanotubes +Antibody +casein. Spectra were obtained between 0.05 Hz – 100 kHz. Amplitude of Alternative voltage: 10 mV.

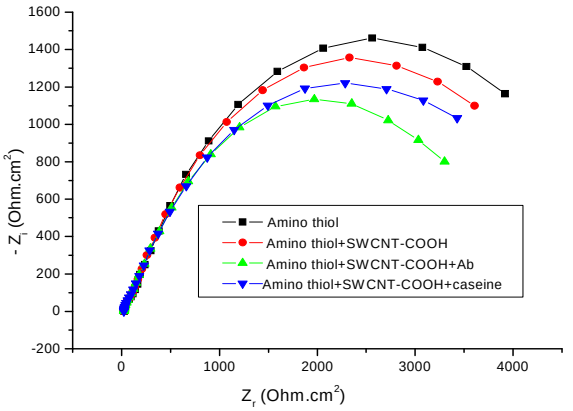

Fig. 4 (b). Nyquist diagram (-Im (z) vs. Re (z)) for the impedance measurements (at -0.4 V) vs. SCE in PBS solution (pH 7.0) corresponding to the various layers grafted onto the gold electrode: (a) Amino thiol; (b) Amino thiol + carbon nanotubes; (c) Amino thiol+ carbon nanotubes +Antibody; (d) Amino thiol +carbon nanotubes +Antibody +casein. Spectra were obtained between 0.05 Hz – 100 kHz. Amplitude of alternative voltage: 10 mV.

The impedance spectra were fitted with an equivalent electrical circuit, shown in Fig. 5a which gives an excellent fit to the experimental data. This equivalent electrical circuit consists of resistive and capacitive elements: Rs is the solution resistance, Rf is the PPy/SWCNT film resistance, Cf is the PPy/SWCNT film capacitance, The constant phase element CPE is then related to the space charge capacitance at the immunosensor layer /electrolyte interface, Rct is related to the charge transfer resistance at the immunosensor layer /electrolyte interface, The constant phase element W is the

Warburg impedance due to mass transfer to the electrode surface.

For the second system, we used the EIS to control the building-up of the biofilm in the PBS (pH 7.0) at -0.4 V potential. Fig. 4b shows the results of impedance spectroscopy measurements as Nyquist plots, for the assembly of the biofilm on gold electrode.

The results show a decrease of the interfacial impedance after carbon nanotubes immobilization reflecting the attachment of the carbon nanotubes on amino thiol and their conducting properties, then the Nyquist plot shows a decrease of the interfacial impedance after antibody immobilization. The increase of CNT conductance was already observed after adsorption of negatively charged protein, this protein being placed inside the Debye length. In our case, the antibody used is in a reduced form, its small dimensions allow its location inside Debye length. A little increase of the interfacial impedance is observed after casein addition, due to the fact that the big size of casein.

The impedance spectra were fitted with a Randles circuit, shown in Fig. 5b which gives an excellent fit to the experimental data. This equivalent electrical circuit consists of resistive and capacitive elements: Rs is the solution resistance, the constant phase element CPE is then related to the capacitance of the biofunctionalized SWCNT-COOH gold electrode/electrolyte interface. CPE reflects the non-ideality of the double-layer at the biofunctionalized SWCNT-COOH gold electrode/electrolyte interface due to the roughness and porosity of the biofilm. Rct is related to the charge transfer resistance at the biofunctionalized SWCNT-COOH gold electrode/electrolyte interface, the constant phase element W is the Warburg impedance, due to mass transfer to the electrode surface.

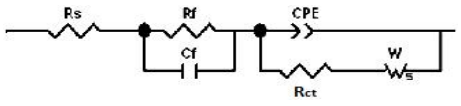

(a)

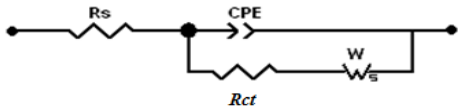

(b)

Fig. 5. (a): Equivalent circuit for the system based on polypyrrole. (b): Randles equivalent circuit for the system based on amino thiol.

3.5. Response of the Immunosensor to D-Dimer

Before the immobilization of the antibody, the biosensor was tested by addition of antigen (D-dimer), no change in the impedance spectrum was observed.

Then the electrode modified with anti-D-dimer antibody fragment was equilibrated with a range of concentrations of the specific antigen D-dimer from 0.1 pg/mL to 5µ g/mL (0.53 fM to 0.26 M).

Antigen–antibody interactions were monitored using impedance spectroscopy in PBS solution (pH 7.0). The impedance spectra obtained after addition of different concentrations of antigen (D-dimer) are shown as Nyquist plots, in Fig. 6a and 6b, where Zr is the real part and Zim is the imaginary part of the complex impedance Z.

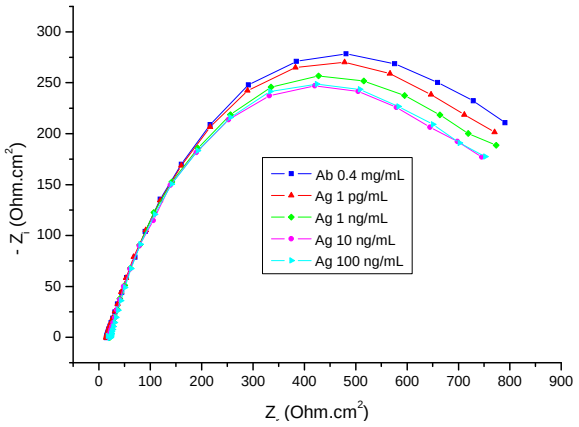

Fig. 6 (a). Nyquist diagram (-Im(z) vs. Re(z)) at -1.2 V vs. SCE in PBS solution pH 7.0) obtained for the impedance measurement on modified gold electrode with polypyrrole film under various concentrations of antigen: (a) 0.4 mg/ml antibody; (b) 1 pg/ml antigen; (c) 1 ng/ml antigen; (d) 10 ng/ml antigen; (e) 100 ng/ml antigen. Spectra were obtained between 0.05 Hz – 100 kHz. Amplitude of Alternative voltage: 10 mV.

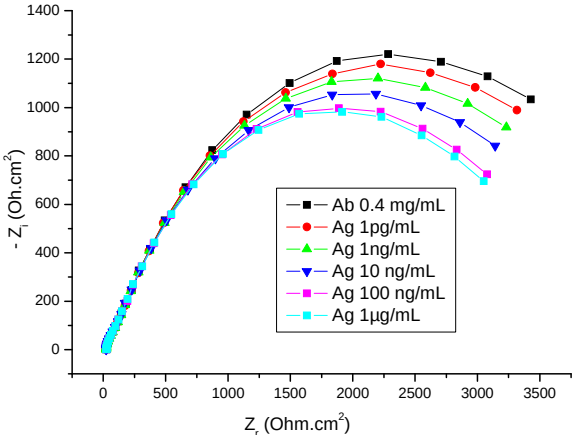

Fig. 6 (b). Nyquist diagram (-Im(z) vs. Re(z)) at -0.4 V vs. SCE in PBS solution pH 7.0) obtained for the impedance measurement on modified gold electrode with amino thiol under various concentrations of antigen: (a) 0.4 mg/ml antibody; (b) 1 pg/ml antigen; (c) 1 ng/ml antigen; (d) 10 ng/ml antigen; (e) 100 ng/ml antigen; (f) 1µg/ml antigen. Spectra were obtained between 0.05 Hz – 100 kHz. Amplitude of Alternative voltage: 10 mV.

Immediately, at low frequencies, the impedance modulus |Z(f)| decreases clearly with the increase of D-dimer concentration, which indicates that a larger amount of D-dimer interacts with the biofunctionalized surface. This reaction leads to a decrease in the electron transfer resistance. The increase of CNT conductivity could be explained by the increase of the negative charge of the immunecomplex which would induce an increase of CNT conductivity.

In order to quantify the immunosensor response, the calibration curves corresponding to the variation of the charge transfer resistance Rct vs. concentrations of D-dimer in PBS solution, is presented in Fig. 7a and 7b for both systems based on polypyrrole and amino thiol respectively.

From the fitted data (Table 1, Table 2), the immunosensor calibration curve presents a linear relation between Rct and the logarithm of D-dimer concentration (C) ranging from 1 pg/mL to 10 ng/mL with a low detection limit of 1 pg/mL for the first system based on polypyrrole and from 1 pg/mL to 100 ng/mL with a low detection limit of 1 pg/mL for the second system based on amino thiol.

If we compare to the results obtained with polypyrrole modified macroelectrodes: detection limit (0.1 ng/mL or 0.53 pM), linearity (up to 10 ng/mL or 53 pM), response time (45 min) [16], we can deduce that the use of SWCNT-COOH modified macroelectrodes lead to a lower detection limit and a higher saturation limit. In the case of polypyrrole modified electrodes.

Table 3 indicates the sensitivity, the detection limit, as well as the dynamic measurement of each immunosensor. Consequently, these results show well that the Immunosensor based on amino thiol is more sensitive that immunosensor based on polypyrrole because it shows the greatest variation of resistance with the best dynamic measurements.

For studying the repeatability of both immunosensor, we repeated this experience with four different immunosensors for both systems. A relative standard deviation of 10.6 % was obtained for the first system with polypyrrole and of 8 % for the second system with amino thiol which proves the repeatability of both systems.

From these results we can compare two methods of immobilization of proteins and conclude that the covalent binding is better and more stable than the adsorption.

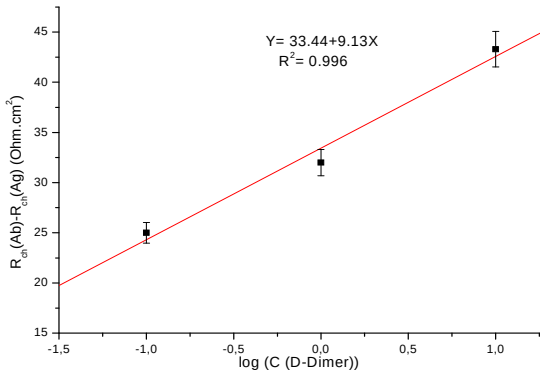

(a)

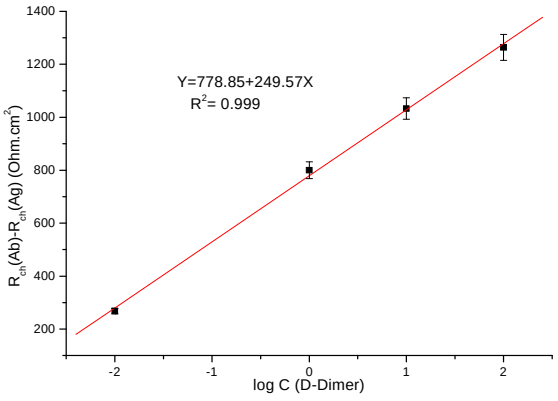

(b)

Fig. 7. (A): Calibration curves describing the variation of charge transfer resistance ΔR_{ct} against D-dimer concentration for immunosensor based on polypyrrole film. (B): Calibration curves describing the variation of charge transfer resistance ΔR_{ct} against antigen concentration for immunosensor based on amino thiol.

The immunosensor was tested in heparinized rat blood spiked with 1 ng/mL (5.3 pM) of D-dimer. The impedance spectra obtained differ from those obtained in PBS of less than 10 %. There was no detectable interference from heparinized rat blood components.

Table 1. Fitting parameters obtained from the proposed equivalent circuit for detection with the immunosensor based on polypyrrole.

Potential (mV)	Ag Concentration	Rs (Ωcm^2)	Rf (Ωcm^2)	Cf (Fcm^2)	Rct	W (Ωcm^2)	CPE (Fcm^2)-	α_{CPE}	$\chi 2$
-1.2 V	0	33.27	12.307	0.0001571	1024	2684	$3.70E^{-5}$	0.826	0.001
	1 pg/mL	34.25	12.503	7.819E-5	1008.8	2329	$3.69E^{-5}$	0.833	0.0012
	1 ng/mL	35.51	18.997	0.00019151	992	2256	$3.51E^{-5}$	0.839	0.0021
	10 ng/mL	33.97	29.51	0.00027161	980.7	2315	$3.83E^{-5}$	0.831	0.001

Table 2. Fitting parameters obtained from the proposed equivalent circuit for detection with the immunosensor based on amino thiol.

Potential (mV)	Ag Concentration	Rs (Ωcm^2)	Rct	W (Ωcm^2)	CPE (Fcm^2)-	α_{CPE}	χ^2
- 0.4 V	0	21.16	4800	3989	$4.53E^{-5}$	0.839	0.0019
	1 pg/mL	20.28	4532	3958	$4.07E^{-5}$	0.813	0.0011
	1 ng/mL	20.73	4343	3569	$4.14E^{-5}$	0.829	0.0009
	10 ng/mL	21.25	3767	3473	$3.94E^{-5}$	0.862	0.0011
	100.ng/mL	19.52	3536	3759	$3.31E^{-5}$	0.802	0.00093

Table 3. Sensitivity, detection limit and the dynamic measurements of immunosensors responses.

	Sensitivity ($Ohm/ng.ml^{-1}$)	Detection limit	Dynamic range	R^2
Immunosensor based on polypyrrole	26	1 pg/ml	1pg/ml – 10 ng/ml	0.9963
Immunosensor based on amino thiol	76	1 pg/ml	1 pg/ml – 100 ng/ml	0.9992

4. Conclusion

In this study, we have developed two methods for fabrication of Immunosensors based on carbon nanotubes for the detection of DVT. The first one consists of immobilizing the carbon nanotubes on polypyrrole film by adsorption and the second one consists of immobilizing the carbon nanotubes on amino thiol by covalent attachment.

From calibration curves, we have demonstrated that the immunosensor based on amino thiol has exhibited a linear relation between Rct and the D-dimer concentrations ranging from 1 pg/mL to 10 ng/mL with a detection limit of 1 pg/mL and a sensitivity of 26 $Ohm.cm^2$, and the immunosensor based on polypyrrole has exhibited a linear relation between Rct and the D-dimer concentrations ranging from 1 pg/mL to 100 ng/mL with a detection limit of 1 pg/mL and a sensitivity of 76 $Ohm.cm^2$.

From these results we can conclude that the covalent binding is better and more stable that the adsorption.

Acknowledgements

The authors thank CAMPUS for support through PHC Maghreb program No. 12 MAG 088 and UTIQUE Project No. 13G 1205. S. Bourigua thanks Rhone-Alpes Region for MIRA grant.

References

[1]. H. R. Buller, A. J. Ten Cate-Hoek, A. W. Hoes, M. A. Joore, K. G. Moons, R. Oudega, Safely ruling out deep venous thrombosis in primary care, *Ann Intern Med*., Vol. 150, 2009, pp. 229-235.

[2]. B. K. Mahmoodi, R. T. Gansevoort, N. J. Veeger, A. G. Matthews, G. Navis, H. L. Hillege, Microalbuminuria and risk of venous thromboembolism, *JAMA*, Vol. 301, 2009, pp. 1790-1797.

[3]. H. Bounameaux, P. de Moerloose, A. Perrier, G. Reber, Plasma measurement of D-dimer as diagnostic aid in suspected venous thromboembolism: an overview, *Thrombosis and Haemostasis,* Vol. 71, 1994. pp. 1–6.

[4]. S. Iijima, Helical microtubules of graphitic carbon, *Nature,* Vol. 354, 1991, pp. 56-58.

[5]. P. M. Ajayan, O. Z. Zhou, Applications of Carbon Nanotubes, *Top. Appl. Phys,* Vol. 80, 2001, pp. 391-425.

[6]. M. M. Treacy, T. W. Ebbesen, T. M. Gibson, Exceptionally high Young's modulus observed for individual carbon nanotubes, *Nature,* Vol. 381, 1996, pp. 678-680.

[7]. A. Peigney, C. Laurent, E. Flahaut, R. R. Bacsa, A. Rousset, Specific surface area of carbon nanotubes and bundles of carbon nanotubes, *Carbon,* Vol. 39, 2001, pp. 507-514.

[8]. R. H. Baughman, A. A. Zakhidov, W. A. de Heer, Carbon nanotubes – the route toward applications, *Science,* Vol. 297, 2002, pp. 787–792.

[9]. L. Dai, A. W. H. Mau, Controlled synthesis of modification of carbon nanotubes and C60: carbon nanostructures for advanced polymeric composite materials, *Adv. Mater*, Vol. 13, 2001, pp. 899–913.

[10]. S. Cosnier, M. Holzinger, Design of carbon nanotube-polymer frameworks by electropolymerization of SWCNT-pyrrole derivatives, *Electrochemica Acta,* Vol. 53, 2008, pp. 3948-3954.

[11]. G. Han, J. Yuan, G. Shi, F. Wei, Electrodeposition of polypyrrole/multiwalled carbon nanotube composite films, *Thin Solid Films,* Vol. 474, 2005, pp. 64-69.

[12]. M. Omastova, M. Trchova, J. Kovarova, J. Stejskal, Synthesis and structural study of polypyrrole prepared in the presence of surfactants, *Synth Met,* Vol. 138, 2003, pp. 447–455.

[13]. S. P. Armes, Optimal reaction conditions for the polymerization of pyrrole by iron (III) chloride in aqueous solution, *Synth. Met,* Vol. 20, 1987, pp. 365–371.

[14]. R. E. Myers, Chemical oxidative polymerization as a synthetic route to electrically conducting polypyrroles, *J. Electron Mater,* Vol. 15, 1987, pp. 61–69.

[15]. J. Ouyang, Y. Li, Great improvement of polypyrrole films prepared electrochemically from aqueous solutions by adding nonaphenol polyethyleneoxy (10) ether, *Polymer*, Vol. 38, 1997, pp. 3997-3999.

[16]. I. Hafaid, S. Chebil, H. Korri-Youssoufi, F. Bessueille, A. Errachid, Z. Sassi, Z. Ali, A. Abdelghani, N. Jaffrezic-Renault, Effect of electrical conditions on an impedimetric immunosensor based on a modified conducting polypyrrole, *Sensors and Actuators B*, Vol. 144, 2010, pp. 323–331.